An actin-like gene can determine cell polarity in bacteria

Zemer Gitai*, Natalie Dye, and Lucy Shapiro*

Department of Developmental Biology, Stanford University, Stanford, CA 94305

Contributed by Lucy Shapiro, April 13, 2004

Achieving proper polarity is essential for cellular function. In bacteria, cell polarity has been observed by using both morphological and molecular markers; however, no general regulators of bacterial cell polarity have been identified. Here we investigate the effect on cell polarity of two cytoskeletal elements previously implicated in cell shape determination. We find that the actin-like MreB protein mediates global cell polarity in *Caulobacter crescentus*, although the intermediate filament-like CreS protein influences cell shape without affecting cell polarity. MreB is organized in an axial spiral that is dynamically rearranged during the cell cycle, and MreB dynamics may be critical for the determination of cell polarity. By examining depletion and overexpression strains, we demonstrate that MreB is required both for the polar localization of the chromosomal origin sequence and the dynamic localization of regulatory proteins to the correct cell pole. We propose that the molecular polarity inherent in an actin-like filament is translated into a mechanism for directing global cell polarity.

The bacterium *Caulobacter crescentus* is particularly well suited to studies of cell polarity because of its inherently asymmetric life cycle that yields, at each cell division, progeny that have different polar morphologies and cell fates (Fig. 1C). The larger "stalked" cell progeny has a cytoplasmic extension known as a stalk at one pole, and the smaller "swarmer" cell progeny has a flagellum and pili at one pole. Immediately after cell division, the stalked cell initiates DNA replication, grows, and synthesizes a flagellum and a pilus secretion apparatus at the pole opposite the stalk before dividing asymmetrically (1). After emerging from a brief G1 arrest, the swarmer cell sheds its flagellum and pili, develops a stalk at that same pole, and initiates DNA replication. This new stalked cell then proceeds through the same asymmetric life cycle as other stalked cells. The stalk is clearly identifiable by light microscopy, making it easy to monitor *Caulobacter* polarity throughout the cell cycle. In addition, several structural and regulatory proteins as well as the origin of replication have been shown to dynamically localize to the stalked pole, the swarmer pole, or both poles during the cell cycle (2). These proteins and chromosomal regions serve as molecular markers of cell polarity. Subcellularly localized molecules are not unique to *Caulobacter*. For example, chemoreceptors, histidine kinases, response regulators, and several chromosomal loci have specific addresses in a wide variety of bacteria, including those without obvious morphological asymmetry (3–7). In addition, virtually every eukaryotic cell has subcellularly localized proteins, such as secretory molecules localized to the bud tip in yeast and neurotransmitter receptors localized to neuronal synapses (8, 9).

The mechanism by which *Caulobacter* cells achieve such exquisite polarity is unknown, and no global regulators of cell polarity have been identified in any bacteria. We approached this problem by searching for mechanisms analogous to those used by eukaryotic cells. Cytoskeletal systems play a key role in virtually every eukaryotic cell polarity event examined (10, 11). *Caulobacter* has three identified cytoskeletal proteins: FtsZ, a tubulin homolog (12, 13); MreB, an actin homolog (14, 15); and CreS, an intermediate filament homolog (16). The assembly of a FtsZ ring at the division plane plays a critical role in cell division but does not appear to regulate cell polarity (17, 18). Meanwhile, MreB has been shown to have a profound effect on cell shape in bacteria such as *Escherichia coli*, *Bacillus subtilis*, and *Caulobacter* (14, 19, 20), and CreS has an effect on cell shape in *Caulobacter* (16). Here we examine the localization dynamics of MreB and the roles of MreB and CreS in cell polarity.

Methods

Bacterial Strains and Plasmids. *C. crescentus* strains CB15N and derivatives were grown in peptone-yeast extract media supplemented with the appropriate combinations of antibiotics, glucose, and xylose (21). For the *mreB* depletion strain, PCR was used to generate an in-frame deletion containing only the first 36 and last 36 bases of the *mreB* gene (CC1543) flanked on either side with 500 bases of homology. This product was subcloned into the pNPTS138 integration vector (gift from M. R. K. Alley, Anacor Pharmaceuticals, Palo Alto, CA), and the resulting construct (LS3807) was transferred by conjugation into CB15N. A cosmid containing the entire *Caulobacter mreB* operon (gift from C. Stephens, Santa Clara University, Santa Clara, CA) was then introduced, and the resulting strain was grown in the presence of 3% sucrose to select for excision of the deletion construct. Strains containing a deleted chromosomal copy of *mreB* were identified by PCR. A *Pxyl*::*mreB* construct was generated by inserting the 2-kb region upstream of the xylose locus in front of the full-length *mreB* gene in the pMR10 low-copy plasmid (22), with an *Nde*I site engineered at the ATG (LS3808). This *Pxyl*::*mreB* plasmid was introduced into the Δ*mreB* strains harboring the *mreB* cosmid. The cosmid was then competed away by introducing an incompatible plasmid, pH1JI (gift from M. R. K. Alley), in the presence of 0.3% xylose. The resulting *mreB* depletion strain (LS3809, *mreB2*) contained a chromosomally deleted *mreB* gene and the *Pxyl*::*mreB* plasmid. For all depletion experiments, this strain was initially grown with 0.03% xylose and then depleted by being grown in 0.2% glucose. For the recovery experiments, *mreB* depletion strains were grown in 0.2% glucose for 24 h followed by 4 h in 0.3% xylose. *mreB* overexpression strains were generated by introducing the *Pxyl*::*mreB* in pMR10 plasmid into CB15N (LS3810). For overexpression experiments, strains were grown in 0.2% glucose and then induced by being grown in 0.3% xylose. Cells were washed twice in the appropriate media whenever shifted and never allowed to enter stationary phase.

creS (CC3699) was deleted by using PCR to generate an in-frame deletion containing only the first 36 and last 36 bases of the *creS* gene flanked on either side with 500 bases of homology. This product was cloned into the pNPTS138 integration vector (LS3811), and the resulting construct was transferred by conjugation into CB15N. This strain was grown in the

Abbreviations: DIC, differential interference contrast microscopy; FISH, fluorescence *in situ* hybridization.

See Commentary on page 8510.

*To whom correspondence may be addressed. E-mail: shapiro@cmgm.stanford.edu or zgitai@stanford.edu.

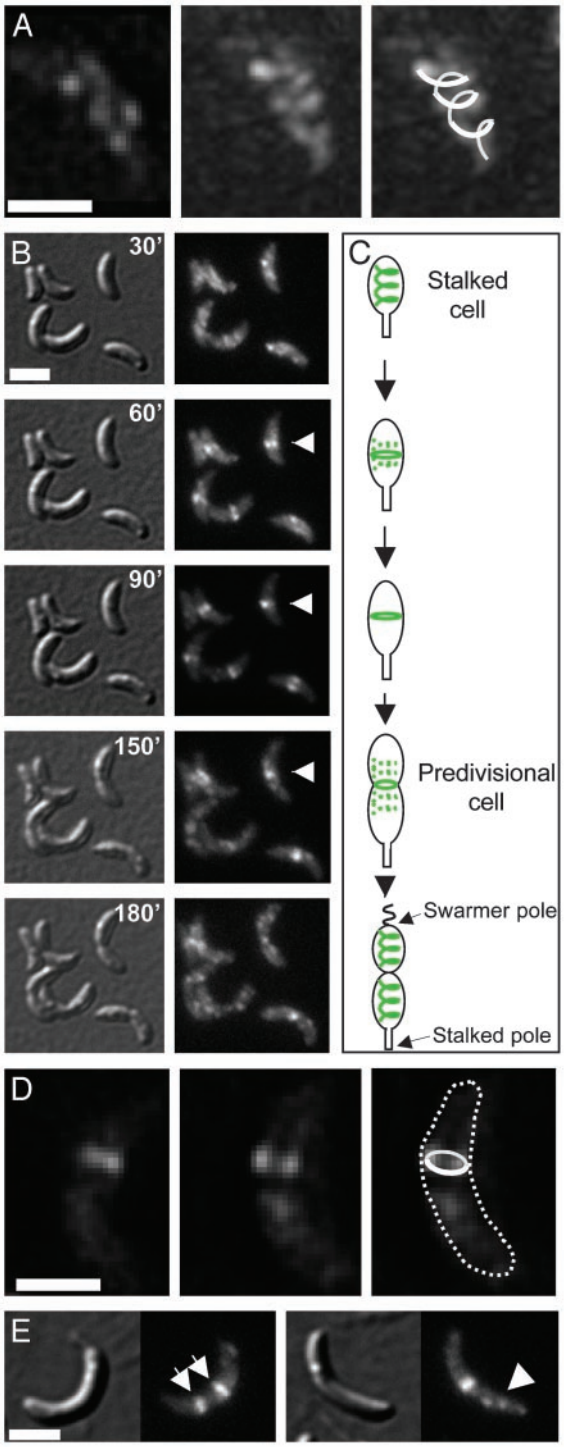

Fig. 1. MreB forms a dynamically contracting and expanding spiral. (*A*) The spiraled pattern of a deconvolved volume projection of MreB-GFP in a stalked cell is shown. (*Left*) A single deconvolved optical section shows a regular pattern of dots on alternating sides of the cell. (*Center*) The entire spiral is seen in the volume projection of 15 optical slices. (*Right*) A cartoon interpretation of the spiral pattern is overlaid on the image from *Center*. (*B*) Time-lapse images of the same MreB-GFP producing cells at 30-min intervals as they progress through cell division. For each time point, images were taken with DIC (*Left*) and GFP fluorescence (*Right*). Arrowheads point to the contracting MreB ring in the three middle panels. (*C*) Schematic of the dynamic behavior of MreB-GFP during the *Caulobacter* cell cycle. (*D*) The division plane MreB-GFP is organized into a hollow ring. The ring is visualized as a continuous band in one optical section (*Left*) and as two separate points in an optical section 300 nM deeper into the cell (*Center*). (*Right*) A cartoon representation of the ring and cell outline is overlaid on the image from *Center*. (*E*) DIC images (*Left*) and GFP fluorescence images (*Right*) of MreB-GFP in strains that have been overexpressing *mreB* for 6 h. The arrows point to two MreB rings found in the same cell, and the arrowhead points to uncontracted MreB in a cell with an MreB ring. (Scale bars, 1 μm.)

presence of 3% sucrose to select for excision of the deletion construct, and strains containing the *creS* deletion (LS3812, *creS2*) were identified by PCR.

MreB-GFP was generated by cloning the full-length *mreB* coding region in frame downstream of GFP in pXGFP4-C1 (LS3813). This *Pxyl*::*gfp-mreB* construct was integrated into the *xylX* locus in the *Caulobacter* chromosome (LS3814) and induced with 0.03% xylose for 2 h to image MreB-GFP. PleC-GFP, CckA-GFP, and DivK-GFP were introduced into the *mreB* depletion, *mreB* overexpression, and *creS* deletion strains by introducing previously described pMR20 based plasmids (LS3338, LS3377, and LS3331) containing each gene fused to GFP and driven by its endogenous promoter, except for PleC-GFP, which is driven by the constitutive *Lac* promoter (23–25). DivJ-GFP was introduced by using ΦCr30 phage transduction to transduce in a previously described *Caulobacter* DivJ-GFP chromosomal fusion (24). Standard molecular biology techniques were followed for all subcloning (26). PCR reactions were performed with the Expand Long Template PCR kit from Roche. All oligonucleotide sequences used are available upon request.

Immunoblots. Immunoblots were carried out as described (27). Protein levels were normalized by loading the equivalent number (0.1) of OD units in each lane. Samples were run on a 10% SDS polyacrylamide gel. The antibodies recognizing PleC, DivJ, CckA, and DivK were used at dilutions of 1:2,000, 1:10,000, 1:10,000, and 1:10,000, respectively (23–25, 28).

Microscopy and Time-Lapse Imaging. All samples were imaged on 1% agarose pads as described (27). For time-lapse experiments, *Pxyl*::*gfp-mreB* strains were induced with 0.03% xylose for 2 h and then synchronized by isolating swarmer cells as described (29). Swarmer cells were grown at room temperature on 1% agarose pads containing 0.03% xylose, and differential interference contrast microscopy (DIC) and fluorescence images of the same field were collected at 30-min intervals. Deconvolution microscopy was performed with a Delta Vision (Applied Precision, Seattle) optical sectioning microscope. Live *Caulobacter* cells were mounted on a polylysine coated slide, and 15 images were collected at 0.1-μm intervals through the sample. The images were deconvolved and made into a volume projection with software provided by the manufacturer.

Results and Discussion

MreB-GFP Is Dynamically Localized into a Contracting and Expanding Spiral. Given that *Caulobacter* displays such dynamic polarization, we characterized the localization dynamics of MreB to gain insight into its possible activities. GFP was fused to the N terminus of MreB, because N-terminal GFP fusions to MreB homologs have been reported to be functional in *B. subtilis* and *E. coli* (30, 31). Deconvolution microscopy on live cells revealed that *Caulobacter* MreB-GFP is organized into a spiral consisting of three to four turns along the length of the cell in stalked and swarmer cells (Fig. 1*A*). This finding is in agreement with a recent immunofluorescence study demonstrating the spiral organization of *Caulobacter*'s endogenous MreB (14).

In *E. coli* and *B. subtilis*, MreB homologs are also organized into a spiral that extends along the long axis of the cell. *B. subtilis* has three MreB homologs (MreB, Mbl, and MreBH), whereas *E. coli* and *Caulobacter* each have only one MreB homolog (19).

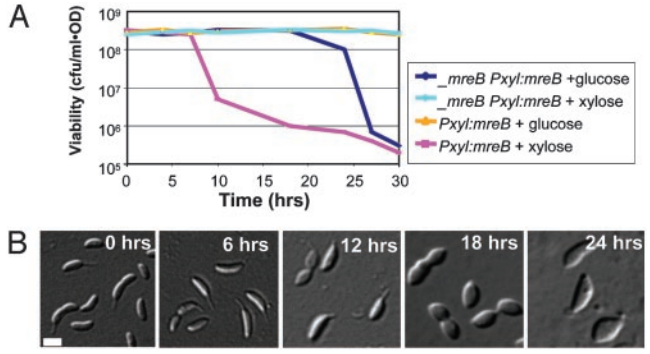

Fig. 2. *mreB* is essential and affects cell shape. (*A*) Viability of *mreB* depletion (Δ*mreB Pxyl*::*mreB)* and overexpression (*Pxyl*::*mreB*) strains after shifts from growth in permissive to nonpermissive media (see *Methods*). (*B*) DIC light microscopy images of *mreB* depletion strains grown in glucose for up to 24 h. (Scale bar, 1 μm.)

Interestingly, the organization of the *Caulobacter* MreB spiral closely resembles that of the *B. subtilis* MreB spiral, with both proteins forming a tight spiral of three to four turns per cell. In contrast, the organization of the *E. coli* MreB spiral resembles that of the *B. subtilis* Mbl spiral, each forming a looser spiral of only one to two turns per cell (19, 31). Thus, the specific evolutionary relationships between the different *mreB* homologs remain unclear, although the general organization of all MreB proteins is conserved.

By using time-lapse imaging of synchronized *Caulobacter* cells expressing MreB-GFP, we were able to follow MreB dynamics in individual cells as they progressed through the cell cycle (Fig. 1 *B* and *C*). Surprisingly, the subcellular localization of *Caulobacter* MreB changed throughout the cell cycle. In stalked cells, the MreB spiral extends along the entire length of the cell. As the cell grows, the MreB spiral appears to condense, localizing to an increasingly restricted zone and ultimately forming a tight ring positioned at the future plane of cell division. Enrichment of MreB at the division plane has also been observed by immunofluorescence (14). Deconvolution microscopy confirmed that the MreB-GFP at the division plane forms a hollow ring (Fig. 1*D*). During cell division, as the cells start to pinch in at the site of the MreB ring, the zone of MreB localization begins to expand; by the time cell division is complete, a spiral of MreB is found along the entire length of both daughter cells (Fig. 1 *B* and *C*).

MreB contraction could be part of a mechanism to find and localize the proper division plane, which is a particularly complex problem in the off-center division of *Caulobacter*. The role of MreB in cell division could involve cooperation with FtsZ, given that FtsZ promotes the formation of division-plane MreB rings (14). In *E. coli* and *B. subtilis*, medial division sites are defined by the Min proteins (32). However, Min homologs are not found in *Caulobacter*. The fact that *E. coli* and *B. subtilis* have other ways to find the division plane may explain why they do not contract their MreB spirals during the cell cycle (19, 30, 31).

It is striking that the dynamic localization of polarity markers occurs concurrently with the dynamic rearrangement of a cytoskeletal structure, such as MreB. In contrast, CreS intermediate filament localization is specific to the crescent face of the cell and does not change during the *Caulobacter* cell cycle (16). In efforts to disrupt MreB dynamics, we tested the effect of overproducing untagged MreB on the distribution of MreB-GFP. In these cells, MreB was still found in a spiral in stalked and swarmer cells, but the tight condensation of MreB into one ring at the division plane was disrupted. MreB was either condensed incompletely or condensed into multiple rings (Fig.

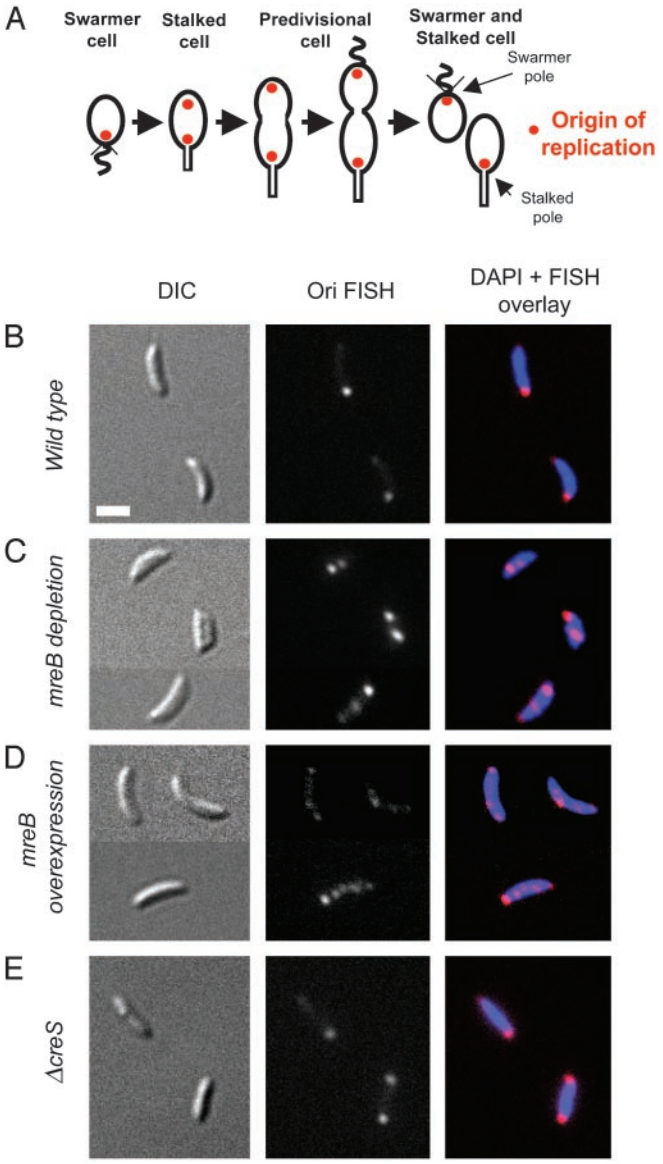

Fig. 3. *mreB* affects the localization and number of origins of replication. (*A*) Schematic representing the localization of the origin(s) of replication at each stage of the cell cycle of wild-type *Caulobacter*. (*B–E*) Shown are representative images from wild-type cells (*B*), cells with *mreB* depleted for 24 h (*C*) or *mreB* overexpressed for 6 h (*D*), or cells in which *creS* was deleted (*E*). For each cell type, images were taken with DIC light microscopy (*Left*), origin FISH fluorescence (*Center*), and an overlay of origin FISH fluorescence (red) and 4′,6-diamidino-2-phenylindole (DAPI) staining (blue) (*Right*). (Scale bar, 1 μm.)

1*E*). In wild-type MreB-GFP cells, 18 ± 4% of a mixed population of cells had one tight division plane ring, whereas in cells overexpressing *mreB* only 4 ± 3% of all cells had one tight ring. Whereas no wild-type cells had more than one tight ring, 7 ± 4% of the cells overexpressing *mreB* had two or more MreB-GFP rings (Fig. 1*E*). *mreB* overexpression thus disrupts the dynamics of MreB cellular organization.

Both MreB and CreS Affect Cell Shape. To determine the role of MreB in cell polarity, we constructed an *mreB* depletion strain. Deleting the *mreB* gene was possible only if the strain also contained a plasmid bearing the *mreB* gene under the control of a xylose-inducible promoter (33) and was grown in the presence of xylose. Depletion of *mreB* strongly affected viability after ≈27

Table 1. MreB disrupts the localization of DNA and protein polarity markers

		mreB depletion			*mreB* overexpression		
	Wild type	0 h	24 h	Recovered	0 h	6 h	Δ*creS*
Origin FISH	87	95	40	—	75	38	87
PleC-GFP	80 (sw)	79	28	43(st), 32 (sw), 8 (b)	83	19	85
DivJ-GFP	82 (st)	72	37	26 (st), 30 (sw), 10 (b)	75	20	78
CckA-GFP	90 (b)	81	22	79 (b)	83	29	88
Divk-GFP	76 (b)	79	33	70 (b)	72	17	80

The numbers shown reflect the percentage of cells that exhibit properly localized foci of FISH or GFP fluorescence. Cells exhibiting additional or misplaced foci were counted as mutant. For the *mreB* depletion strain, percentages are shown for cells grown in permissive xylose media (0 h), cells grown for 24 h in nonpermissive glucose media, and cells grown for 24 h in nonpermissive glucose media followed by 4 h in permissive xylose media (Recovered). For the *mreB* overexpression strain, percentages are shown for cells grown in permissive glucose media (0 h) and cells grown for 6 h in nonpermissive xylose media. Letters in parentheses designate at which pole the focus was found: sw, swarmer pole; st, stalked pole; b, both poles. No designation is given for the origin FISH, because the origin is found at different poles at different stages in the cell cycle. When only one number is given, all cells with foci had foci localized to the same pole or poles. When multiple numbers are given, they represent the percentage of cells with foci at each pole. At least 80 cells were scored for each condition, and the standard error of the proportion ranged from 3% to 5% for all conditions.

h of growth in the absence of xylose, thereby confirming that *mreB* is an essential gene (Fig. 2*A*) (14). Consistent with its previously known role in cell shape maintenance in *E. coli*, *B. subtilis,* and *Caulobacter* (14, 19, 20), depletion of *mreB* for several hours caused a severe impact on cell shape. These *Caulobacter* cells lost their normal crescentoid shape and took on varied morphologies before cell death: predominantly first ellipsoid, then spherical, and finally amorphous (Fig. 2*B*). By introducing the plasmid containing *mreB* under the control of the xylose promoter into wild-type *Caulobacter*, we also constructed a strain in which *mreB* could be overexpressed. *mreB* overexpression for >8 h affected viability (Fig. 2*A*), but had no obvious effect on cell shape (Fig. 3*D*; see also Fig. 4).

CreS is a coiled-coil protein capable of polymerizing into filaments similar to intermediate filaments (16). It has been shown that *creS* mutants are viable and exhibit a cell shape defect (16). We generated an in-frame deletion of the *creS* gene and confirmed that cells carrying this *creS* allele are viable, with a straight, rod-like morphology unlike the normal crescentoid shape of *Caulobacter* (Fig. 3*E*; see also Fig. 4).

Origin Localization Is Disrupted in *mreB* but Not *creS* Mutants. Recent studies in a wide variety of bacteria have demonstrated that chromosomal regions are reproducibly and dynamically localized within the cell (34). Chromosome positioning therefore represents an informative marker for cell polarity. We have focused on the *Caulobacter* origin of replication, which is dynamically localized during the cell cycle. In wild-type swarmer cells, the origin DNA sequence is always localized to the swarmer pole (Fig. 3*A*) (35). Once the swarmer cell differentiates into a stalked cell and initiates DNA replication, one copy of the origin is rapidly moved to the opposite pole (Fig. 3*A*) (35). We assessed the impact of depleting *mreB,* overexpressing *mreB,* and deleting *creS* on cell polarity by using a 10-kb fluorescence *in situ* hybridization (FISH) probe to examine the location of the *Caulobacter* origin of replication in each of these strains (35).

When *mreB* was depleted for 24 h or overexpressed for 6 h, the polar localization of the origins of replication was dramatically disrupted. Although cells were still viable at these time points, the origins were misplaced (Fig. 3 *C* and *D* and Table 1). Many of the mutant cells also exhibited multiple foci (Fig. 3 *C* and *D*). This phenotype is consistent with a defect in cell division resulting in the accumulation of multiple origins: In the media used, wild-type cells would replicate their DNA every 90 min, and the mutant cells never exhibited more origins than expected replication events. The presence of multiple and misplaced origins in *mreB* mutants could also suggest a defect in chromosome segregation. This scenario is consistent with observations in *E. coli* and *B. subtilis* (36, 37). Although the origins may form looser foci in some cells overexpressing *mreB*, the origin always appeared as a tight focus in the *mreB* depletion strains, suggesting that MreB does not play an essential role in chromosome condensation (Fig. 3 *C* and *D*).

Polar localization of the origins was not disrupted in abnormally shaped *creS* deletion cells (Fig. 3*E*). Origin number and condensation also appeared unaffected in *creS* deletion strains (Fig. 3*E*). Because the origins can be mislocalized in normally shaped cells overexpressing *mreB* and properly localized in misshapen *creS* cells, origin localization is separable from cell shape.

Polar Proteins Are Mislocalized in *mreB* but Not *creS* Mutants. The presence of MreB in a lengthwise spiral in early stalked cells, the stage during which the newly replicated origin is rapidly moved to the distal pole, is consistent with MreB acting to mediate chromosome movement. However, MreB could also function to localize a protein factor which is in turn needed to localize the origin of replication. It is also possible that MreB functions to dictate the *Caulobacter*'s global polarity information. To explore this possibility, we examined the impact of *mreB* mutants on the locations of known polar proteins.

Here, we have focused on four proteins: three integral membrane histidine kinases (PleC, DivJ, and CckA) and a cytoplasmic single-domain response regulator (DivK). Each of these proteins plays a different role in the cell cycle, dynamically localizes to different cell poles at different times in the cell cycle, and is for the most part independently localized (Fig. 4*A*) (2). PleC regulates the biogenesis of the stalk and pili and is localized to the swarmer pole in swarmer and predivisional cells (24, 38). DivJ regulates cell division as well as the placement and length of the stalk; it is localized to the stalked pole in all cell types with a stalk (24, 39). CckA regulates cell division, DNA replication, and the assembly of the polar flagellum and pili. In predivisional cells, CckA is found at both poles (25). DivK regulates stalk formation, cell division, and DNA replication and is localized to the stalked pole in early stalked cells and to both poles in predivisional cells (23, 40). DivK is unable to localize in the absence of DivJ (23), but of the other combinations tested, each of these four proteins can be assembled at their proper poles in the absence of the others (2, 41).

As compared to wild-type cells, *mreB* depletion for 24 h significantly disrupted the localization of all four of the GFP

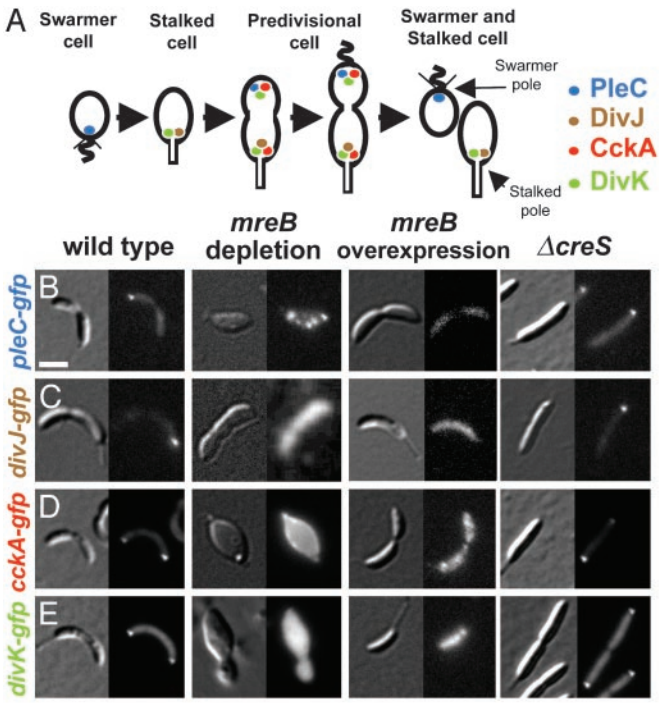

Fig. 4. MreB affects the localization of PleC, DivJ, CckA, and DivK. (*A*) Schematic representing the localization of PleC (blue), DivJ (brown), CckA (red), and DivK (green) at each stage in the cell cycle of wild-type *Caulobacter*. (*B–E*) Representative images from cells expressing PleC-GFP (*B*), DivJ-GFP (*C*), CckA-GFP (*D*), and DivK-GFP (*E*). Shown are wild-type cells, cells with *mreB* depleted for 24 h or *mreB* overexpressed for 6 h, or cells in which *creS* was deleted. For each cell, images shown were taken with DIC light microscopy (left image) and GFP fluorescence (right image). (Scale bar, 1 μm).

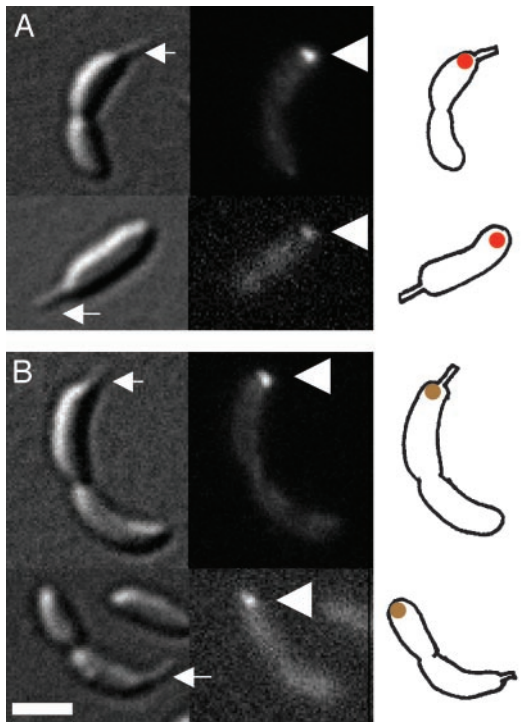

Fig. 5. MreB determines *Caulobacter* polarity. DIC (*Left*, left image), GFP fluorescence (*Left*, right image), and cartoon depictions (*Right*) of recovered *mreB* depletion strains expressing PleC-GFP (*A*) or DivJ-GFP (*B*). These cells have been grown in glucose for 24 h to deplete *mreB* and then shifted for 4 h into xylose-containing media to restore *mreB* expression. The arrows point to the stalked pole, and the arrowheads point to the GFP foci. (Scale bar, 1 μm.)

fusions to PleC, DivJ, CckA, and DivK (Fig. 4 *B–E* and Table 1). In each case, the GFP fusions in these misshapen cells appeared either highly diffuse or localized to many puncta localized around the entire cell (Fig. 4 *B–E*). To examine protein localization in cells with proper cell shape but disrupted MreB dynamics, we examined the location of these normally polar proteins in cells overexpressing *mreB*. Overexpression of *mreB* for 6 h had a severe effect on the localizations of all four GFP fusions to PleC, DivJ, CckA, and DivK, resulting in each case in a diffused or evenly dispersed localization (Fig. 4 *B–E* and Table 1). Western blots showed that PleC, DivJ, CckA, and DivK levels were not dramatically perturbed by *mreB* depletion or overexpression (data not shown), ruling out the possibility that MreB influences the polar localization of PleC, DivJ, CckA, and DivK by affecting their concentrations.

Such striking effects of both depleting and overexpressing *mreB* on multiple polarity markers implicate MreB as a general regulator of *Caulobacter* polarity. In addition, because *mreB* overexpression disrupts both MreB localization dynamics and cell polarity, MreB's dynamic rearrangement may be critical for determining proper polarity. The mechanism by which MreB mediates polar localization remains unclear, given that MreB could act to either initiate or maintain localization. MreB could also act either directly or indirectly. For example, actin can directly traffic proteins (8); however, MreB can influence the assembly of the peptidoglycan cell wall and could, in turn, affect landmarks necessary for correct protein localization (14, 42).

Unlike MreB depletion or overexpression, deletion of *creS* had no impact on the localization of the polarity markers examined. Although these cells have an altered shape (rod-like instead of crescentoid), they still grow stalks at one pole, allowing their stalked and swarmer poles to be identified. As compared with wild-type, GFP fusions to PleC, DivJ, CckA, and DivK were all localized to their proper poles in *creS* deletion mutants (Fig. 4 *B–E* and Table 1). Given that polar markers are mislocalized in the normally shaped *mreB* overexpressors and correctly localized in the abnormally shaped *creS* deletions, the localization of both DNA and protein polarity markers can be uncoupled from cell shape.

MreB Determines *Caulobacter* Polarity. To determine whether depleting *mreB* permanently damages the cells, we examined the reversibility of its effects on protein localization. We started with *mreB* depletion strains carrying *mreB* under the control of the xylose promoter and expressing GFP fusions to PleC, DivJ, CckA, or DivK. Growth of these cells for 24 h in glucose-containing media depleted *mreB* and delocalized PleC, DivJ, CckA, and DivK (Fig. 4 and Table 1). We then let these cells replenish their levels of MreB by growing them for an additional 4 h in xylose-containing media to induce *mreB* expression. After these 4 h, the PleC, DivJ, CckA, and DivK GFP fusions were all restored to clear polar foci found at frequencies indistinguishable from wild type (Table 1). The rapid reversibility of mislocalization is consistent with MreB directly affecting protein localization.

Surprisingly, although the recovered PleC-GFP and DivJ-GFP cells did recover foci, the subcellular localization of these foci differed markedly from that of wild type. PleC-GFP is normally found in one focus at the swarmer pole. Of the cells that recovered a clear PleC-GFP focus, roughly half had a single focus at the swarmer pole, whereas the other half had a single focus at the opposite, stalked pole (Table 1 and Fig. 5*A*). DivJ-GFP is normally found in one focus at the

stalked pole. Of the cells that recovered a clear DivJ-GFP focus, roughly half had a single DivJ-GFP focus at the stalked pole, whereas the other half had a single DivJ-GFP focus at the opposite, swarmer pole (Table 1 and Fig. 5*B*). A minority of both the PleC-GFP and DivJ-GFP recovered cells had foci at both poles (Table 1). It is unclear whether the stalks in these recovered cells are newly formed, such that we cannot establish whether stalk placement is MreB-independent. We were unable to assess whether the localization of CckA and DivK is randomized because they are normally located at both poles.

This disruption of the correct placement of two different polar markers could be due to a randomization of the cell's polarity. Alternatively, many of the recovered cells with correctly localized PleC and DivJ could represent cells that never delocalized these proteins during MreB depletion. In this scenario, the majority of the recovered foci would be at the incorrect pole. In either case, the appearance of two different polar markers at incorrect poles indicates that cells that have lost and then regained MreB do not retain memory of their polarization before depletion. Thus, MreB is not just permissively required for polar localization but contains the polarity information to direct PleC and DivJ to specific poles.

We hypothesize that the MreB spiral is a polarized structure and that PleC and DivJ (or their upstream localization factors) are trafficked toward opposite ends of that polar structure. When the MreB spiral is reconstituted after depletion, it reassembles into a polarized spiral, but, lacking MreB-dependent polarity cues, it randomly orients itself relative to the stalk. This reconstituted spiral would still deliver PleC and DivJ to opposite poles, but would randomize the pole to which they are delivered, potentially explaining our results. Because the swarmer pole eventually matures into a stalked pole, a polarized MreB spiral could not simply be cut in half, as it would end up oppositely oriented with respect to the old and new stalked poles. The transient condensation of the MreB spiral into a ring may provide a mechanism to orient a newly formed spiral such that correct polarity is maintained. The need to reorganize MreB would also explain why manipulations, such as *mreB* overexpression, that disrupt MreB dynamics also disrupt cell polarity.

Conclusion

We have shown that the actin-like MreB protein contains the polarity information to determine subcellular localization. In addition, MreB dynamically rearranges itself from a spiral to a ring and back into a spiral, and these dynamics may be required for proper polarity. Although the specific mechanisms by which MreB acts have yet to be identified, our findings allow us to now examine specific molecular models for how bacterial polarity is determined. Moreover, the striking use of the actin cytoskeleton for regulating polarity in both prokaryotes and eukaryotes suggests that the deep conservation between these groups extends beyond individual proteins to entire cellular processes.

We thank Sherry Wang for advice, reagents, and assistance in performing the FISH analysis and Todd Blankenship, Joseph Chen, Sean Crosson, Ellen Judd, Patrick McGrath, Coleen Murphy, Sean Murray, Ann Reisenauer, Martin Thanbichler, and Patrick Viollier for comments and advice. Z.G. is supported by the Stanford Genomics Postdoctoral Fellowship.

1. Jensen, R. B., Wang, S. C. & Shapiro, L. (2002) *Nat. Rev. Mol. Cell. Biol.* **3,** 167–176.
2. Jacobs-Wagner, C. (2004) *Mol. Microbiol.* **51,** 7–13.
3. Ryan, K. R. & Shapiro, L. (2003) *Annu. Rev. Biochem.* **72,** 367–394.
4. Teleman, A. A., Graumann, P. L., Lin, D. C., Grossman, A. D. & Losick, R. (1998) *Curr. Biol.* **8,** 1102–1109.
5. Lam, H., Matroule, J. Y. & Jacobs-Wagner, C. (2003) *Dev. Cell* **5,** 149–159.
6. Maddock, J. R. & Shapiro, L. (1993) *Science* **259,** 1717–1723.
7. Niki, H., Yamaichi, Y. & Hiraga, S. (2000) *Genes Dev.* **14,** 212–223.
8. Pruyne, D. W., Schott, D. H. & Bretscher, A. (1998) *J. Cell Biol.* **143,** 1931–1945.
9. Rongo, C., Whitfield, C. W., Rodal, A., Kim, S. K. & Kaplan, J. M. (1998) *Cell* **94,** 751–759.
10. Etienne-Manneville, S. & Hall, A. (2002) *Nature* **420,** 629–635.
11. Drubin, D. G. & Nelson, W. J. (1996) *Cell* **84,** 335–344.
12. Quardokus, E., Din, N. & Brun, Y. V. (1996) *Proc. Natl. Acad. Sci. USA* **93,** 6314–6319.
13. Lowe, J. & Amos, L. A. (1998) *Nature* **391,** 203–206.
14. Figge, R. M., Divakaruni, A. V. & Gober, J. W. (2004) *Mol. Microbiol.* **51,** 1321–1332.
15. van den Ent, F., Amos, L. A. & Lowe, J. (2001) *Nature* **413,** 39–44.
16. Ausmees, N., Kuhn, J. R. & Jacobs-Wagner, C. (2003) *Cell* **115,** 705–713.
17. Bi, E. F. & Lutkenhaus, J. (1991) *Nature* **354,** 161–164.
18. Quardokus, E. M., Din, N. & Brun, Y. V. (2001) *Mol. Microbiol.* **39,** 949–959.
19. Jones, L. J., Carballido-Lopez, R. & Errington, J. (2001) *Cell* **104,** 913–922.
20. Wachi, M., Doi, M., Okada, Y. & Matsuhashi, M. (1989) *J. Bacteriol.* **171,** 6511–6516.
21. Ely, B. (1991) *Methods Enzymol.* **204,** 372–384.
22. Roberts, R. C., Toochinda, C., Avedissian, M., Baldini, R. L., Gomes, S. L. & Shapiro, L. (1996) *J. Bacteriol.* **178,** 1829–1841.
23. Jacobs, C., Hung, D. & Shapiro, L. (2001) *Proc. Natl. Acad. Sci. USA* **98,** 4095–4100.
24. Wheeler, R. T. & Shapiro, L. (1999) *Mol. Cell* **4,** 683–694.
25. Jacobs, C., Domian, I. J., Maddock, J. R. & Shapiro, L. (1999) *Cell* **97,** 111–120.
26. Sambrook, J., Fritsch, E. & Maniatis, T. (1989) *Molecular Cloning: A Laboratory Manual* (Cold Spring Harbor Lab. Press, Plainview, NY).
27. Ryan, K. R., Judd, E. M. & Shapiro, L. (2002) *J. Mol. Biol.* **324,** 443–455.
28. Viollier, P. H., Sternheim, N. & Shapiro, L. (2002) *EMBO J.* **21,** 4420–4428.
29. Tsai, J. W. & Alley, M. R. (2001) *J. Bacteriol.* **183,** 5001–5007.
30. Carballido-Lopez, R. & Errington, J. (2003) *Dev. Cell* **4,** 19–28.
31. Shih, Y. L., Le, T. & Rothfield, L. (2003) *Proc. Natl. Acad. Sci. USA* **100,** 7865–7870.
32. Errington, J., Daniel, R. A. & Scheffers, D. J. (2003) *Microbiol. Mol. Biol. Rev.* **67,** 52–65.
33. Meisenzahl, A. C., Shapiro, L. & Jenal, U. (1997) *J. Bacteriol.* **179,** 592–600.
34. Sherratt, D. J. (2003) *Science* **301,** 780–785.
35. Jensen, R. B. & Shapiro, L. (1999) *Proc. Natl. Acad. Sci. USA* **96,** 10661–10666.
36. Kruse, T., Moller-Jensen, J., Lobner-Olesen, A. & Gerdes, K. (2003) *EMBO J.* **22,** 5283–5292.
37. Soufo, H. J. & Graumann, P. L. (2003) *Curr. Biol.* **13,** 1916–1920.
38. Wang, S. P., Sharma, P. L., Schoenlein, P. V. & Ely, B. (1993) *Proc. Natl. Acad. Sci. USA* **90,** 630–634.
39. Ohta, N., Lane, T., Ninfa, E. G., Sommer, J. M. & Newton, A. (1992) *Proc. Natl. Acad. Sci. USA* **89,** 10297–301.
40. Hecht, G. B., Lane, T., Ohta, N., Sommer, J. M. & Newton, A. (1995) *EMBO J.* **14,** 3915–3924.
41. Sciochetti, S. A., Lane, T., Ohta, N. & Newton, A. (2002) *J. Bacteriol.* **184,** 6037–6049.
42. Daniel, R. A. & Errington, J. (2003) *Cell* **113,** 767–776.